SMALL INSECT MEASUREMENTS USING A CUSTOM MEMS FORCE SENSOR

M.S. Bartsch[a], W. Federle[b], R.J. Full[c], T.W. Kenny[a]
Stanford University Mechanical Engineering[a], University of Würzburg Behavioral Physiology & Sociobiology[b], University of California at Berkeley Integrative Biology[c]
Phone: (650)723-2279, E-mail: mbartsch@stanford.edu

ABSTRACT

A multi-axis sensor with micro-Newton force resolution has been designed and fabricated for the purpose of studying the biomechanics of insect locomotion. The sensor comprises a rigid central plate supported at each corner by thin beams with piezoresistive transducers sensitive to both normal and in-plane forces. The sensor is configured to measure the instantaneous ground reaction force components produced by insects as large as cockroaches when they step onto the sensor plate during walking or running. This paper describes the results of analytical modeling and finite element simulations used to characterize the performance and mechanical behavior of the sensor microstructure.

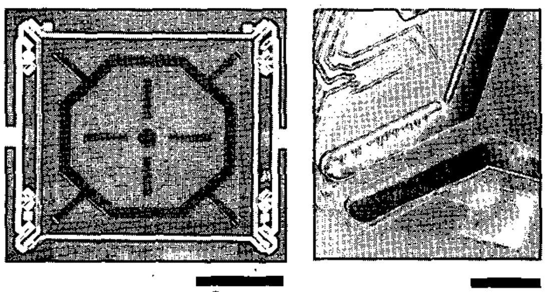

Figure 1: (a) Full sensor element showing central plate with small diagonal flexures at each corner. (b) SEM of a single flexure.

INTRODUCTION

Engineers have used insects like the cockroach as prototypes for the design of biomimetic robots capable of negotiating unstructured terrain at high speed [1,2]. Other insects such as ants provide insight into the biomechanics of climbing and adhesion applicable to progressively smaller robotic systems. In both cases, ground reaction forces, the forces exerted by the feet of a walking organism on a surface, provide key insight into the mechanisms of insect locomotion.

Large-scale force platforms previously available for studying insect ground reaction forces have allowed detailed study of the biomechanics of relatively large, slow insects such as the death-head cockroach *Blaberus discoidalis* [3,4]. However, the measurement bandwidth of this apparatus has made it impractical for studying faster insects like the American cockroach *Periplaneta americana*. Similarly, the force platform design lacks the sensitivity and resolution necessary to study smaller insects such as ants.

To address these performance limitations and expand both the quality and scope of future insect measurements, we have fabricated a custom silicon micromachined force sensor. Like its large-scale predecessor, this sensor is designed to simultaneously measure normal and in-plane single-leg ground reaction force components. Where the older force platform had an effective measurement bandwidth of 118Hz and minimum force resolution on the order of 0.5mN, the MEMS sensor has demonstrated mechanical bandwidth in excess of 1kHz and micro-Newton force resolution or better [5].

SENSOR DESIGN

Reference [5] provides a detailed description of the design, fabrication, and calibration of the multi-axis MEMS force sensor. The device consists of a rigid square central plate 5.3mm on a side which is supported at each corer by flexure beams 555µm long, 70µm wide, and between 20 and 100µm thick. Unless specified, all results presented here refer to 50µm thick flexures. Figure 1a shows a single full sensor element while Figure 1b shows a magnified view of the flexure beam at one corner of the device. Near its anchored end, each flexure has a pair of 200µm long ion-implanted piezoresistive strain gauges, one along the beam centerline and one along its edge. Piezoresistor positions may be inferred from the routing of aluminum interconnects in Figure 1b. The central piezoresistor allows measurement of beam bending in the out-of-plane or normal direction, while the edge piezoresistor senses in-plane or lateral bending. Comparison of the signals in both resistors allows the effect of superimposed normal and lateral loads to be evaluated for each of the four flexure beams.

SENSOR MODELING

Analytical modeling. We have previously formulated an approximate analytical model which is used to resolve piezoresistor voltage signals into ground reaction force components (F_x, F_y, and F_z) independent of the location at which the insect foot contacts the sensor plate. Reference [5] presents a detailed description of the model and a discussion of the simplifying assumptions upon which it relies. Some of these assumptions and approximations are geometric in nature: simpler shapes substitute for more complex forms to allow the application of analytical

TRANSDUCERS '03
The 12th International Conference on Solid State Sensors, Actuators and Microsystems, Boston, June 8-12, 2003

0-7803-7731-1/03/$17.00 ©2003 IEEE

methods such as linear beam theory. Other assumptions serve to simplify the large system of equations needed to relate measured piezoresistor signals to the mechanical response of the sensor structure. In all cases, it is desirable to understand how these approximations are likely to affect model accuracy.

(a)

(b)

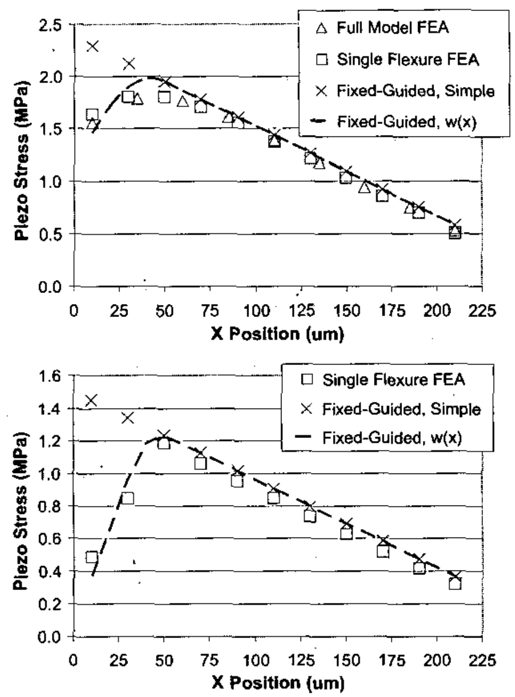

Figure 2: Piezoresistor bending stress profiles as predicted by FEA and analytical fixed-guided beam models. (a) Normal bending. (b) In-plane bending.

Finite element modeling. While analytical methods are generally preferable for reducing experimental data, finite element analysis (FEA) provides a powerful tool for characterizing the mechanical behavior of geometrically complex structures like the MEMS sensor. As a result, FEA represents an ideal method for testing and evaluating the approximations inherent to the analytical model formulation. FEA results may also be used to refine the analytical model, reducing potential sources of error and improving accuracy. This becomes particularly important with respect to in-plane force measurement where the analytical model is most susceptible to modeling errors.

Toward this end, we have created and tested two basic FEA models. The first simulates the mechanical behavior of the entire sensor structure, while the second provides a more detailed analysis of the mechanics of an individual flexure beam. Solid models are created in ANSYS and auto-meshed using simple tetrahedral elements with manual mesh refinement as needed. For both models, a series of key-points are positioned on the flexures to coincide with the position of piezoresistors in the actual device. Other key-points provide sites for repeatable application of loads and tracking of structural deformation and deflection.

SINGLE FLEXURE FEA RESULTS

Stress analysis. Based on sensor geometry and the structural constraints imposed on the flexure elements, the analytical model treats flexures as fixed-guided beams where the root end is fixed and the plate end guided (free to translate but not rotate). For small deformations, this approach should reasonably approximate actual flexure mechanics. Given its role in the analytical model, the fixed-guided approximation must effectively capture two aspects of flexure mechanics: the force/stress response of the beam, and its force/deflection characteristics.

The stress experienced by a the mid-line piezoresistor on a fixed-guided flexure subject to a normal load is given as

$$\sigma_z(x) = \frac{M_z(x)\frac{1}{2}t}{\frac{1}{12}wt^3} = \frac{6(R_z L/2 - R_z x)}{wt^2} \qquad (1)$$

Here L, w, and t are the nominal length, width, and thickness of the beam, $M_z(x)$ is the bending moment, and R_z is the out-of-plane component of the force transmitted to the flexure by the sensor plate. A similar expression describes the stress produced in a flexure-edge piezoresistor due to bending under an in-plane load.

While equation (1) assumes a beam of uniform cross-section, the width of the actual flexure varies somewhat due to the fillet at its root. Figure 2 compares the piezoresistor stress profiles predicted by the fixed-guided model with those obtained from FEA simulations of both normal and in-plane load cases. In Figure 2a, a 1mN central load applied to the full sensor FEA model provides a single-flexure force equivalent to a 0.25mN normal loading of the single-flexure FEA model with appropriate displacement constraints applied.

As Figure 2 shows, the simple fixed-guided beam model yields a reasonably good prediction of piezoresistor stress outside the region where w is variable. While somewhat suspect in a rigorous sense, modifying the fixed-guided model of equation (1) to treat width as a function of x yields stress profile predictions which better approximate the FEA results as shown in Figure 2.

Because piezoresistor output voltage depends on the average stress along the length of the resistor, evaluation of average stress predictions may provide the best gauge of the effectiveness of the fixed-guided beam model. Considering the single-flexure FEA model as the basis of comparison, Table 1 summarizes the error in predicting average piezoresistor stress associated with each model described so far. Correcting for width variations appears to enhance the accuracy of the fixed-guided stress prediction, but errors are still sizable. This result is understandable given that linear beam theory is predicated at least in part on the assumption that the beams it models have constant cross-sections. To address these errors, correction factors derived from the FEA results may need to be incorporated into future iterations of the analytical model.

Deflection analysis. The fixed-guided beam model also relates flexure force to displacement. For a load R_z coupled through the sensor plate to a given flexure, the deflection of the plate end of that flexure is

$$\delta_z = -\frac{R_z L^3}{Ewt^3} \quad (2)$$

where E is Young's Modulus. Rearranging this formula as a ratio of force to displacement yields the normal stiffness K_n of the flexure. A comparable equation describes in-plane deformation and stiffness K_i. Table 2 summarizes the flexure normal and in-plane stiffness predicted by the fixed-guided model as well as full-sensor and single-flexure finite element results. For normal stiffness, beam theory agrees quite well with the full sensor FEA, but both appear to over-predict flexure stiffness compared with the single flexure FEA model. Conversely, FEA results describe a beam which is stiffer in-plane than fixed-guided estimates would suggest. Most likely this reflects the effect of variation in the beam cross-section along the length of the flexure.

FULL SENSOR FEA RESULTS

Normal loading. As noted above, the sensor is designed to reproduce insect foot force components independent of foot placement. FEA of the full sensor model provides insight into how sensor behavior and performance vary spatially with load position. Figure 3 shows out-of-plane stiffness as a function of position where the corners of the plot correspond to the corners of the sensor plate. This "local stiffness" is obtained by applying a 1mN load at various points on the plate, then calculating stiffness based on the displacement of the loading point. In this case, normal stiffness varies from a maximum of 38kN/m at the plate center to 18kN/m near the plate corners, a 53% variation.

This result begs the question whether normal force sensitivity also shows a comparable spatial variation across the sensor. To check force sensitivity, we first invoke a summation of normal forces acting on the plate

$$\sum F_{Z-axis} = 0 = F_z + R_{Az} + R_{Bz} + R_{Cz} + R_{Dz} \quad (3)$$

where F_z is the normal foot force component and R_{Az} through R_{Dz} are the out-of-plane reactions exerted on the plate corners by each flexure beam. As equation (1) suggests, the reaction force R_{Az} of a flexure is linearly proportional to its average piezoresistor stress, $\sigma_{Az\text{-}avg}$. As a result, we may rearrange and restate equation (3) as

$$F_z \propto \sigma_{Az-avg} + \sigma_{Bz-avg} + \sigma_{Cz-avg} + \sigma_{Dz-avg} \quad (4)$$

This simplification provides a method for gauging the spatial uniformity of normal force sensitivity

Table 1: Average piezoresistor stress model errors

Model	Normal % Error	In-plane % Error
Single flexure FEA	0%	0%
Full sensor FEA	-1%	Na
Fixed-guided, simple	+11.3%	+24.8%
Fixed-guided, w(x)	+5.4%	+9.7%

Table 2: Comparison of flexure stiffness model results

Normal Model	K_n (N/m)	% Error
Single flexure FEA	9.11x10^3	0%
Full sensor FEA	9.71x10^3	+6.6%
Fixed-guided model	9.72x10^3	+6.7%
In-Plane Model	**K_i (N/m)**	**% Error**
Single flexure FEA	2.20x10^4	0%
Fixed-guided model	1.91x10^4	-13.2%

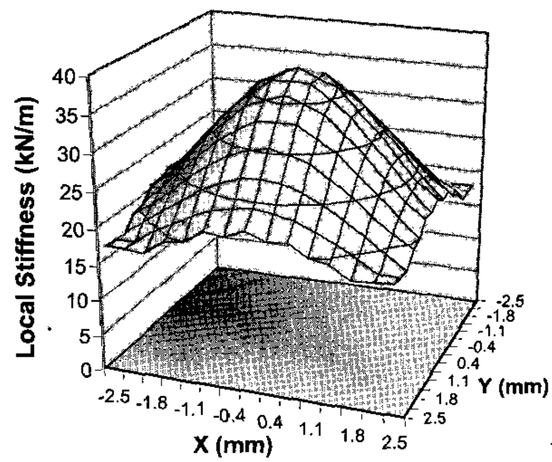

Figure 3: Spatial variation in local normal stiffness

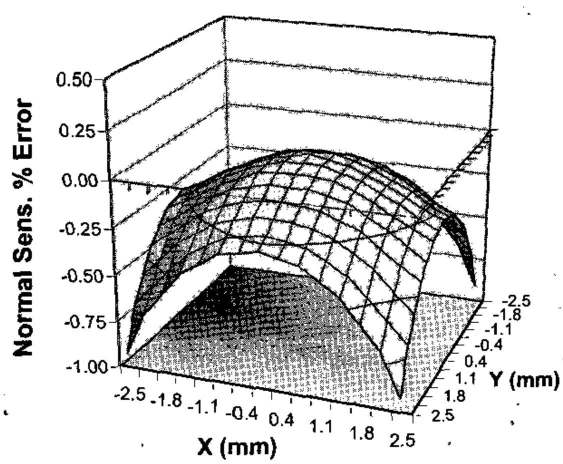

Figure 4: Normal force sensitivity variations, % error computed with respect to sensitivity at plate center.

decoupled from any inaccuracies which may be present in flexure beam theory models. Provided that the sum of the four average mid-flexure piezoresistor stresses remains constant as 1mN loads are applied to different locations on the sensor, normal force sensitivity will also be constant. Figure 4 shows the results of such an FEA experiment where average piezoresistor sums are normalized to the central load sum. As the plot shows, sensitivity varies by less than 1% across the sensor plate.

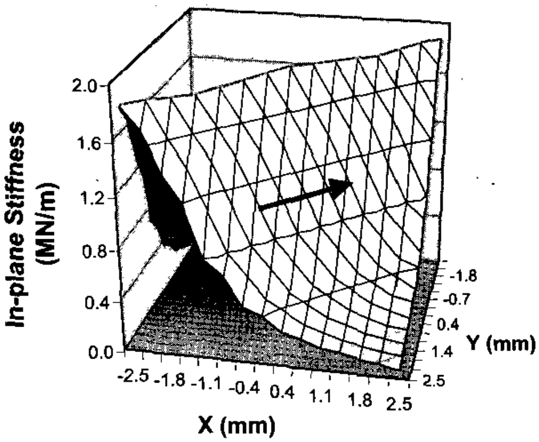

Figure 5: Spatial variation of local in-plane stiffness. The arrow indicates the direction of the applied force

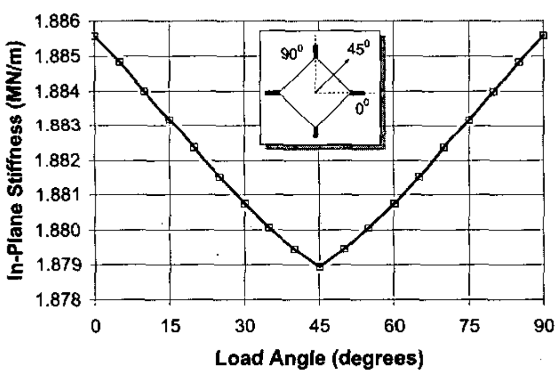

Figure 6: Angular variation of in-plane stiffness with respect to a rotated central load.

In-plane loading. The full-sensor finite element model also allows characterization of the comparatively complex in-plane mechanics of the sensor structure. Following the method described for normal loads in Figure 3, Figure 5 shows the local stiffness relative to a 1mN in-plane load oriented parallel to one diagonal of the sensor plate and applied at various locations. Again, stiffness is calculated based on the displacement of the loading point in the direction of the load. In this case, stiffness along the axis of the flexures is nearly 1.9×10^6N/m, while stiffness near the root of the perpendicular flexures drops to just under 9×10^4N/m. This factor of 20 variation reflects the difference between axial and transverse flexure stiffness.

In-plane stiffness may also be evaluated by applying a 1mN force to the center of the plate, then rotating that force through an arc of 45 degrees or more. Again, stiffness is determined by the displacement of the load point in the direction of the applied force. Figure 6 shows that the absolute angular variation of in-plane stiffness determined by this method never exceeds 0.4% of its on-axis value.

CONCLUSIONS & FUTURE WORK

Preliminary finite element modeling results have yielded important insights about the MEMS force sensor design and the analytical model which describes it. Notably, the single-flexure FEA model has identified significant discrepancies between fixed-guided beam bending predictions and the corresponding finite element models. Full-sensor FEA results have demonstrated that while apparent normal stiffness may vary across the sensor, overall normal force sensitivity remains essentially uniform. Similarly, for a centrally applied load, the in-plane stiffness of the sensor shows negligible angular variation.

Future work will focus on applying FEA results to refine the existing analytical model. With modeling errors minimized, our ability to extract meaningful in-plane force measurements from insect experimental data will be greatly improved. These model enhancements will enable the first ever true multi-axis single-leg ground reaction force measurements of insects smaller than cockroaches.

ACKNOWLEDGEMENTS

This work has been supported by a Department of Defense NDSEG Fellowship, the National Science Foundation "XYZ on a Chip" program, and the Office of Naval Research Multi-University Research Initiative. Devices were fabricated at the Stanford Nanofabrication Facility, part of the National Nanofabrication Users Network supported by the NSF through award number ECS9731294.

REFERENCES

[1] E. Ritzman, R. D. Quinn, J. T. Watson, and S. N. Zill, "Insect walking and biorobotics: a relationship with mutual benefits," *Bioscience*, vol. 50, no. 1, pp. 23-33, 2000.

[2] J. G. Cham, S. A. Bailey, J. E. Clark, R. J. Full, and M. R. Cutkosky, "Fast and robust: hexapedal robots via shape deposition manufacturing," *Intl. J. Robotics Res.*, Accepted for Publication, Dec. 2001.

[3] R. J. Full and M. S. Tu, "Mechanics of six-legged runners," *J. exp. Biol.*, vol. 148, pp. 129-146, 1990.

[4] R. J. Full, R. Blickhan, and L. H. Ting, "Leg design in hexapedal runners," *J. exp. Biol.*, vol. 158, pp. 369-390, 1991.

[5] M.S. Bartsch, W. Federle, R.J. Full, T.W. Kenny, "A multi-axis force sensor for studying insect biomechanics," *JMEMS*, Submitted 25 July, 2002.